EPJ Web of Conferences **297**, 01015 (2024) https://doi.org/10.1051/epjconf/202429701015
ISNA23

The slow neutron-capture process in stars

Diego Vescovi[1,2,*]

[1]INAF – Osservatorio Astronomico d'Abruzzo, via Mentore Maggini snc, I-64100, Teramo, Italy
[2]INFN – Sezione di Perugia, via Alessandro Pascoli snc, I-06123, Perugia, Italy

Abstract. Most elements heavier than iron in the Universe are produced through neutron captures. The solar system abundance distribution indicates that they were created primarily in two nucleosynthetic processes, the slow and the rapid processes. Here, we cover the fundamental aspects of the s-process. The ever-growing amount of information gathered from astronomical observations and analyses of stardust grains recovered from meteorites provides tight constraints on the mechanisms of the s-process and where it occurs. Comparison of chemical abundance patterns with stellar model predictions clearly identifies evolved low-mass and massive stars as the s-process astrophysical sites.

1 Introduction

The synthesis of elements beyond iron primarily occurs through mechanisms other than charged particle reactions [1, 2]. Specifically, it involves the slow (s) and rapid (r) neutron-capture processes [3, 4], which are influenced by factors such as the neutron density, the neutron-capture reaction rate, and the decay rate of the synthesized isotopes. Relatively low neutron densities are achieved during core-He burning and shell-C burning in massive stars or the thermally-pulsing phase of asymptotic giant branch (AGB) stars [5, 6]. In contrast, high neutron densities arise during the explosive phase of supernovae or compact binary merger events [4].

The distinction between the s- and r- processes lies in the timescale relative to the corresponding β decay. In the *s*-process, neutron capture occurs over a timescale longer than the corresponding β decay, causing the *s*-process path in the nuclide chart to consistently evolve near the beta stability valley. On the contrary, the *r*-process operates on timescales shorter than β-decay timescales, leading the path to deviate significantly from the stability valley and produce strongly β-unstable nuclei, extending up to the neutron drip line. These nucleosynthesis processes result in abundance peaks for nuclei with more stable configurations, in correlation with the positions of the neutron shell closures at neutron numbers $N = 50, 82, 126$ (see Figure 1). The separation in abundance peaks within mass ranges A=80-90, 130-140, and 190-210 makes clear the action of two different neutron-capture processes.

2 The s-process

Under the assumption that only neutron captures and beta decays occur, the equation that expresses the temporal evolution of the number abundance of a nucleus with atomic mass A

*e-mail: diego.vescovi@inaf.it

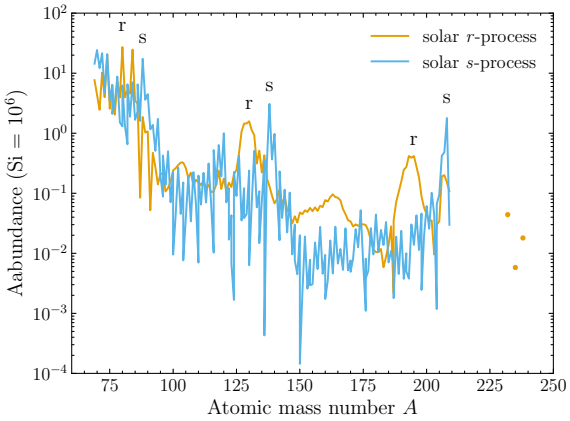

Figure 1. Decomposition of isotopic solar system s-process and r-process abundances as a function of atomic mass number A. Data from [7].

can be written as follows:

$$\frac{dN_A(t)}{dt} = N_{\rm n}(t)\left[-N_A(t)\langle\sigma v\rangle_A + N_{A-1}(t)\langle\sigma v\rangle_{A-1}\right] - \lambda_A N_A(t) \tag{1}$$

where N_A and $N_{\rm n}$ are the number densities of a nucleus A and of free neutrons, respectively; $\langle\sigma v\rangle_A$ is the neutron-capture reaction rate per pair of particles A, and λ_A is the decay rate. In the most general case, the neutron density, the neutron-capture reaction rate and the decay rate are not constant, but depend on the (dynamic) conditions of the stellar environment.

Neutron capture takes place when the term within square brackets is positive and prevails over the decay term. In other words, this condition is met when the difference between these two terms is positive. When a neutron is captured, a product nucleus is formed which, if unstable, decays before capturing another neutron. This translates into the decay term in Equation (1) to prevail. On the contrary, in the case of a stable nucleus, or with a mean lifetime much longer than the average time for neutron capture, it may capture another neutron, producing a heavier isotope. In this case, the decay term is negligible.

In the s-process, a series of neutron captures by a chain of isotopes take place until a radioactive isotope, whose decay probability is significantly higher than the probability of capturing another neutron, is reached ($\lambda_\beta \gg \lambda_{\rm n\gamma} = N_{\rm n}\langle\sigma v\rangle$). Then it decays, subsequently initiating another series of neutron captures. Since the s-process takes place under relatively low neutron density conditions ($N_{\rm n} \sim 10^6 \div 10^{12}$ neutrons cm^{-3}), the time scale for neutron capture is typically much longer than the β-decay time scale of radioactive isotopes, thus explaining the adjective *slow*. As a result, nuclei synthesized through the *s*-process are located along the so-called β-stability valley. Within this framework, the presence of abundance peaks in the solar system s-process abundance pattern is a natural consequence of the small capture cross sections of the neutron magic nuclides. These act as *bottlenecks* for the abundance flow thus accumulating and giving rise to pronounced abundance peaks at strontium (Sr; $A = 88$), barium (Ba; $A = 138$), and lead (Pb; $A = 208$). During the *s*-process nucleosynthesis, specific radioactive isotopes that exhibit a β-decay timescale comparable to that of neutron capture ($\tau_\beta \sim \tau_{\rm n\gamma}$) may cause the nucleosynthesis path to diverge into two branches. The analysis of branching point isotopes is critical in understanding the temperature and neutron density conditions attained during the *s*-process [8, 9].

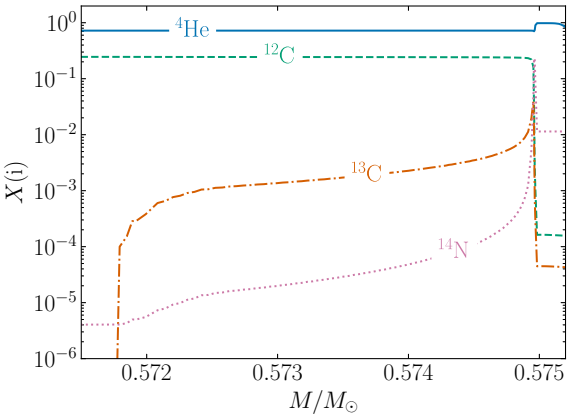

Figure 2. Abundances of selected isotopes in the ^{13}C pocket region after the third TDU in a 2 $M_\odot$ model with solar metallicity (see [12] for details).

The *s*-process nucleosynthesis occurs in two distinct astrophysical environments: massive stars ($M \gtrsim 10\ M_\odot$) and low-mass stars ($1\ M_\odot \lesssim M \lesssim 4\ M_\odot$) during their AGB phase. The first site accounts for the weak *s*-process component of the solar system (the abundances of s-process isotopes with $A \lesssim 90$), while the second one accounts for the main and the strong component ($A \gtrsim 90$) [3, 5, 10, 11]. Neutron capture processes necessitate a continuous supply of free neutrons. For the s-process, the main neutron sources are represented by the ^{22}Ne(α, n)^{25}Mg and the ^{13}C(α, n)^{16}O reactions. The former prevails in massive stars, whereas the latter dominates in AGB stars.

3 AGB stars

The abundance of approximately half of the nuclei beyond strontium is attributed to s-processing in low-mass AGB stars. At this stage, the star has a degenerate C-O core increasing in mass, two active H- and He-burning shells separated by a He-rich intermediate zone in radiative equilibrium (He-intershell), and an expanded H-rich convective envelope. The helium generated by the H-burning shell accumulates, increasing the density and temperature in the innermost zones. Over tens of thousands of years, the He-shell undergoes a thermonuclear runaway, commonly referred to as thermal pulse (TP), rapidly releasing energy that drives convective motions across the He-intershell region. Simultaneously, this causes an expansion and subsequent cooling of the H shell, which eventually quenches, while He burning proceeds in radiative conditions. Subsequently, the star contracts again, heating up and triggering the re-ignition of the H shell. This cycle repeats throughout the thermally pulsing AGB phase until most of the envelope is eroded by stellar winds [13–15].

During envelope expansion, convection penetrates below the H-He discontinuity, beyond the region where the H shell was active. Consequently, convective motions mix fusion by-products to the surface, altering the star's surface abundance distribution — this phenomenon is known as the third dredge-up (TDU). During each TDU, protons are partially mixed into the He intershell due to some phenomena occurring at the base of the envelope. Then, with the re-ignition of the H shell, protons are captured by abundant ^{12}C nuclei via the ^{12}C(p, γ)^{13}N(β^+)^{13}C chain, leading to the formation of a thin layer enriched in ^{13}C, known as the ^{13}C pocket (see Figure 2). Then neutrons are efficiently released during the time elapsing be-

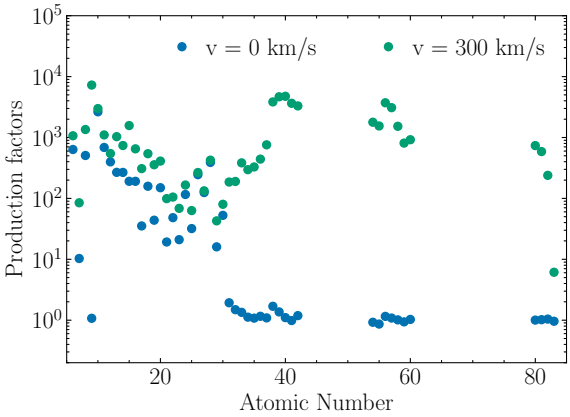

Figure 3. Production factors of the various elements for a 25 $M_\odot$ model with metallicity [Fe/H] = −2. Data from [32].

tween two subsequent pulses, at about 9×10^7 K, through the ^{13}C(α, n)^{16}O reaction [16, 17]. This represents the main neutron source in low-mass AGB stars. Various physical mechanisms inducing the partial mixing of H-rich material from the convective envelope have been explored in the past, including convective overshoot [18, 19], rotation [20, 21], Kelvin-Helmholtz instabilities and internal gravity waves [22, 23], and magnetic fields [12, 24–28]. Despite the substantial progress that has been made in this field, the formation of the ^{13}C pocket represents a major uncertainty in the s-process nucleosynthesis of heavy elements and remains an area of extensive research.

During the interpulse period, due to the outward advance of the H-burning shell, the He intershell becomes significantly enriched in ^{14}N, which is later mixed in the convective zone generated by the TP and converted to ^{22}Ne via the ^{14}N$(\alpha,\gamma)^{18}$F$(\beta^+\nu)^{18}$O$(\alpha,\gamma)^{22}$Ne chain. At sufficiently high temperatures ($T \gtrsim 3 \times 10^8$ K), the ^{22}Ne(α, n)^{25}Mg reaction is efficiently activated. This is the case for intermediate AGB stars ($M \gtrsim 4\ M_\odot$) [29]. In these objects, the ^{13}C pocket, if it forms at all, may be so thin and poor in ^{13}C that it is not relevant for the s-process [30]. Instead, in less massive AGB stars, the ^{22}Ne(α, n)^{25}Mg reaction plays only a marginal role in shaping the final s-element abundance distribution [31].

4 Massive stars

Traditionally, the s-process in massive stars has been acknowledged as the main source of the weak s-process component in the Solar System, encompassing elements between iron and the first s-process peak (Sr, Y, and Zr) [11]. The main neutron source is identified as the ^{22}Ne(α, n)^{25}Mg reaction, predominantly activated during core-He burning and shell-C burning, at temperatures around 3×10^8 K and 10^9 K, respectively [33, 34]. As in low-mass counterparts, ^{22}Ne is produced through the ^{14}N$(\alpha,\gamma)^{18}$F$\,(e^+\nu)^{18}$ O$(\alpha,\gamma)^{22}$Ne reaction chain, from the ^{14}N produced by the action of the CNO cycle in the previous H-burning phase. As a result, the weak s-process component generated in massive stars exhibits a secondary-like behavior, diminishing with decreasing metallicity. After helium exhaustion, some amount of ^{22}Ne survives, and additional neutron production is guaranteed by the α particles supplied by the ^{12}C$(^{12}\mathrm{C},\alpha)^{20}$Ne reaction. The following core-collapse supernova explosion also influences some of the ejected s-process abundances [32]. Finally, when rotation is considered

in a stellar model, the predicted outcomes may be way different. In low-metallicity rotating massive star models, the interaction between the He-burning core and the H-burning shell due to rotation-induced instabilities, leads to the production of a substantial amount of primary ^{14}N, which eventually is converted by alpha captures to (primary) ^{22}Ne. This, in turn, gives rise to a time-integrated neutron flux capable of synthesizing heavy nuclei, extending up to the third s-process peak in the most extreme cases (see Figure 3).

DV acknowledges support from the European Union – NextGenerationEU RFF M4C2 1.1 PRIN 2022 project "2022RJLWHN URKA", the INAF Theory Grant "Understanding R-process & Kilonovae Aspects", and the INAF Minigrant "CHEmical ClockS".

References

[1] E.M. Burbidge, G.R. Burbidge, W.A. Fowler, F. Hoyle, RvMP **29**, 547 (1957)
[2] A.G.W. Cameron, PASP **69**, 201 (1957)
[3] M. Lugaro, M. Pignatari, R. Reifarth, M. Wiescher, ARNPS **73**, 315 (2023)
[4] J.J. Cowan, C. Sneden, J.E. Lawler et al., RvMP **93**, 015002 (2021)
[5] M. Busso, R. Gallino, G.J. Wasserburg, ARA&A **37**, 239 (1999)
[6] S.E. Woosley, A. Heger, T.A. Weaver, RvMP **74**, 1015 (2002)
[7] N. Prantzos, C. Abia, S. Cristallo, M. Limongi, A. Chieffi, MNRAS **491**, 1832 (2020)
[8] S. Bisterzo, R. Gallino, F. Käppeler et al., MNRAS **449**, 506 (2015)
[9] N. Liu, S. Cristallo, D. Vescovi, Universe **8**, 362 (2022), 2206.13721
[10] R. Gallino, C. Arlandini, M. Busso et al., ApJ **497**, 388 (1998)
[11] F. Käppeler, R. Gallino, S. Bisterzo et al., Reviews of Modern Physics **83**, 157 (2011)
[12] D. Vescovi, S. Cristallo, M. Busso, N. Liu, ApJL **897**, L25 (2020), 2006.13729
[13] J. Iben, I., A. Renzini, ARA&A **21**, 271 (1983)
[14] F. Herwig, ARA&A **43**, 435 (2005)
[15] O. Straniero, R. Gallino, S. Cristallo, Nuclear Physics A **777**, 311 (2006)
[16] O. Straniero, R. Gallino, M. Busso et al., ApJL **440**, L85 (1995)
[17] S. Cristallo, M. La Cognata, C. Massimi et al., ApJ **859**, 105 (2018), 1804.10751
[18] F. Herwig, T. Bloecker, D. Schoenberner et al., A&A **324**, L81 (1997)
[19] S. Cristallo, O. Straniero, R. Gallino et al., ApJ **696**, 797 (2009), 0902.0243
[20] F. Herwig, N. Langer, M. Lugaro, ApJ **593**, 1056 (2003), astro-ph/0305491
[21] L. Siess, S. Goriely, N. Langer, A&A **415**, 1089 (2004)
[22] P.A. Denissenkov, C.A. Tout, MNRAS **340**, 722 (2003)
[23] U. Battino, M. Pignatari, C. Ritter et al., ApJ **827**, 30 (2016), 1605.06159
[24] O. Trippella, M. Busso, S. Palmerini et al., ApJ **818**, 125 (2016), 1512.06777
[25] D. Vescovi, M. Busso, S. Palmerini, et al., ApJ **863**, 115 (2018), 1807.01058
[26] D. Vescovi, S. Cristallo, S. Palmerini et al., A&A **652**, A100 (2021), 2106.08241
[27] M. Busso, D. Vescovi, S. Palmerini et al., ApJ **908**, 55 (2021), 2011.07469
[28] L. Magrini, D. Vescovi, G. Casali et al., A&A **646**, L2 (2021), 2101.04429
[29] O. Straniero, S. Cristallo, L. Piersanti, ApJ **785**, 77 (2014), 1403.0819
[30] S. Cristallo, O. Straniero, L. Piersanti, D. Gobrecht, ApJS **219**, 40 (2015), 1507.07338
[31] S. Cristallo, L. Piersanti, O. Straniero et al., ApJS **197**, 17 (2011), 1109.1176
[32] M. Limongi, A. Chieffi, ApJS **237**, 13 (2018)
[33] C.M. Raiteri, R. Gallino, M. Busso, et al., ApJ **419**, 207 (1993)
[34] M. Pignatari, R. Gallino, M. Heil et al., ApJ **710**, 1557 (2010)